Polarization rotation by an rf-SQUID metasurface

J.-G. Caputo,[1,*] I. Gabitov,[2,†] and A. I. Maimistov[3,4,‡]

[1]*Laboratoire de Mathématiques, INSA de Rouen, Avenue de l'Universite, 76801 Saint-Etienne du Rouvray, France*

[2]*Department of Mathematics, University of Arizona, Tucson, Arizona 85704, USA*

[3]*Department of Solid State Physics and Nanostructures, National Research Nuclear University, Moscow Engineering Physics Institute, Kashirskoe sh. 31, 115409 Moscow, Russia*

[4]*Department of Physics and Technology of Nanostructures, Moscow Institute for Physics and Technology, Institutskii Lane 9, Dolgoprudny, 141700 Moscow Region, Russia*

(Received 7 January 2015; revised manuscript received 2 March 2015; published 24 March 2015)

We study the transmission and reflection of a plane electromagnetic wave through a two-dimensional array of rf-SQUIDs. The basic equations describing the amplitudes of the magnetic field and current in the split-ring resonators are developed. These yield in the linear approximation the reflection and transmission coefficients. The polarization of the reflected wave is independent of the frequency of the incident wave and of its polarization; it is defined only by the orientation of the split ring. The reflection and transmission coefficients have a strong resonance that is determined by the parameters of the rf-SQUID; its strength depends essentially on the incident angle.

DOI: 10.1103/PhysRevB.91.115430 PACS number(s): 81.05.Xj, 07.57.Kp

I. INTRODUCTION

Recently a layer of metamaterial containing specially etched designs, referred to as metasurfaces, was used to induce a phase gradient in an incident electromagnetic wave [1]. This leads to a generalized Snell's law and the control of the transverse structure of the wave front [1]. This study was done in the optical domain; it then was extended to microwaves by Shalaev *et al.* [2]. The phase gradient is due to a plasmon resonance between the electromagnetic wave and the designs etched on the surface. Artificial films can also rotate the polarization of an electromagnetic wave, the so-called Faraday rotation. Kodera *et al.* [3] showed that a metamaterial film, containing a periodic array of conductive rings with each an isolator, induces Faraday rotation. All these devices follow the same principle, i.e., a linear resonance occuring between the electromagnetic wave and a plasmonic wave in the film.

A drawback of these devices is that they cannot be used for different frequencies; in particular they cannot be tuned. By construction they are adapted to a specific frequency. It would be useful to have a system whose response could be changed over a significant range of frequencies. Such a device exists; it is a split-ring Josephson resonator (rf-SQUID) [4–7]. The rf-SQUIDs as basic elements of quantum metamaterials were discussed in [8–11,13]. In the experimental study [11,12], it was shown that one can tune the resonance frequency of these devices. It should be pointed that this system has a discrete energy spectrum and a large magnetization [13]. Then the energy of interaction with an external field can be of the order of the transition energy between neighboring energy states.

In this article we show that a film of properly oriented rf-SQUIDs controls the polarization of a wave reflecting on the metasurface. This is similar to a Faraday effect; the wave is strongly reoriented at the resonance. We determine the parameters of the reflected and transmitted waves in the linear approximation. The reflection and transmission coefficients depend on the frequency and on the stationary state of the system. In that sense, the device is active; its parameters can be modified.

II. THE MODEL

We consider a plane wave normally incident on a layer of rf-SQUIDs as shown in Fig. 1; the layer coincides with the (x,y) plane. All the rings in the film are oriented in the same direction given by the normal vector $\mathbf{n}$. The interaction of the individual rf-SQUID with the electromagnetic field is determined by the magnetic flux through the split ring. Therefore the orientation of the rf-SQUID controls the parameters of the transmitted and reflected waves. This orientation is characterized by the angle θ between the magnetic component $\mathbf{H}$ and the normal $\mathbf{n}$ to the split ring. We assume that the film is embedded in a homogeneous dielectric layer. The dielectric permittivity of this medium is ε. The model describing the interaction of electromagnetic field with the system of rf-SQUIDs is based on Maxwell's equations and the equation for the response of the rf-SQUIDs:

$$\nabla \times \mathbf{E} = -(\mu_0 \mathbf{H} + \mathbf{M})_{,t}, \tag{1}$$

$$\nabla \times \mathbf{H} = \varepsilon_0 \varepsilon \mathbf{E}_{,t}, \tag{2}$$

$$\nabla \cdot \mathbf{D} = 0, \quad \nabla \cdot \mathbf{B} = 0 \tag{3}$$

[14]. The magnetization $\mathbf{M}$ in Eq. (1) is localized in the array whose thickness is much smaller than the wavelength λ. Therefore the magnetization can be written as follows:

$$\mathbf{M}(t,\mathbf{r}) = \sum_a \mathbf{m}_a(t)\delta(z) \approx \mathbf{m}(t) n_r l \delta(z), \tag{4}$$

where $\mathbf{m}_a(t)$ are individual rf-SQUID magnetizations, $l \ll \lambda$ is the film thickness, and n_r is the density of rf-SQUID resonators. The vector $\mathbf{m}(t)$ is the magnetic moment of the

*caputo@insa-rouen.fr
†gabitov@math.arizona.edu
‡amaimistov@gmail.com

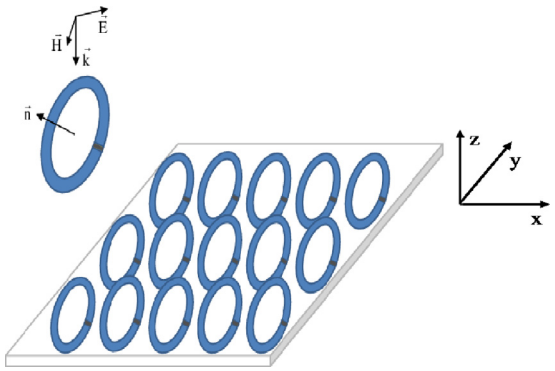

FIG. 1. (Color online) Schematic view of the electromagnetic wave incident on the layer containing split-ring Josephson junction resonators. One ring is shown, indicating the orientation.

rings [7] which we assume to oscillate coherently. From Maxwell's equations (1)–(3) we obtain the wave equation

$$\mathbf{H}_{,tt} - \frac{c^2}{\varepsilon}\Delta\mathbf{H} = -\frac{1}{\mu_0}\mathbf{M}_{,tt}. \tag{5}$$

Since the model considered is translationally invariant with respect to the x axis, this equation can be presented as

$$\mathbf{H}_{,tt} - \frac{c^2}{\varepsilon}\mathbf{H}_{,zz} = -\frac{1}{\mu_0}\mathbf{M}_{,tt}. \tag{6}$$

Let us now consider the Josephson split-ring part. The magnetic moment is

$$\mathbf{m}(t) = SI\mathbf{n}, \tag{7}$$

where I is the current in the loop (11). Combining the two equations (4) and (7) we get the final expression for $\mathbf{M}$,

$$\mathbf{M} = SIn_r l\delta(z)\mathbf{n}. \tag{8}$$

Plugging the above expression into the wave equation (6) yields the wave equation

$$\mathbf{H}_{,tt} - \frac{c^2}{\varepsilon}\mathbf{H}_{,zz} = -\frac{1}{\mu_0}SI_{,tt}n_r l\delta(z)\mathbf{n}. \tag{9}$$

As in [13] the current in the ring is given by

$$I = -L^{-1}(\Phi_e + \Phi_0\varphi), \tag{10}$$

where Φ_e is the flux induced by the electromagnetic field and where L is the inductance of the loop. The variable φ is the superconducting phase in the junction; to simplify the equations we use the reduced flux quantum $\Phi_0 = \frac{\hbar}{2e}$ as unit of flux. The flux Φ_e across the ring of area S is

$$\Phi_e = S\mathbf{H}\cdot\mathbf{n},$$

where $\mathbf{n}$ is the normal vector to the ring. This gives us the current in the ring

$$I = -L^{-1}\left(S\mathbf{H}\cdot\mathbf{n} + \Phi_0\varphi\right). \tag{11}$$

The evolution of the variable φ is the same as in [13] except that the current on the right-hand side is modified. We have

$$C\Phi_0\frac{\partial^2\varphi}{\partial t^2} + \frac{\Phi_0}{R}\frac{\partial\varphi}{\partial t} + I_c\sin\varphi = I. \tag{12}$$

Plugging (11) into (12) and multiplying by L/Φ_0 we recover the rf-SQUID relation (see for example Vol. 2 of [15]):

$$LC\varphi_{,tt} + \frac{L}{R}\varphi_{,t} + \varphi + \frac{LI_c}{\Phi_0}\sin\varphi = -\frac{S}{\Phi_0}\mathbf{H}\cdot\mathbf{n}. \tag{13}$$

Our model consists in the wave equation (9) together with the split-ring Josephson equation (13). These can be normalized as in [13]. The natural units of time, flux, and space are

$$\omega_T = \frac{1}{\sqrt{LC}}, \quad \Phi_0, \quad \lambda_T = \frac{c}{\omega_T\sqrt{\varepsilon}},$$

where ω_T is the Thompson frequency and λ_T is the Thompson wavelength. The magnetic field $\mathbf{H}$ is normalized as

$$\mathbf{h} = \frac{\mathbf{H}S}{\Phi_0}, \quad \tau = \omega_T t, \quad \zeta = \frac{z}{\lambda_T}. \tag{14}$$

In terms of these variables the final equations are

$$\mathbf{h}_{,\tau\tau} - \mathbf{h}_{,\zeta\zeta} = \kappa(\mathbf{h}_{,\tau\tau}\cdot\mathbf{n} + \varphi_{,\tau\tau})\delta(\zeta)\mathbf{n}, \tag{15}$$

$$\varphi_{,\tau\tau} + \alpha\varphi_{,\tau} + \varphi + \beta\sin\varphi = -\mathbf{h}\cdot\mathbf{n}, \tag{16}$$

where the parameters α, β, and κ are

$$\alpha = \frac{1}{R}\sqrt{\frac{L}{C}}, \quad \beta = \frac{LI_c}{\Phi_0}, \quad \kappa = n_r S^2\frac{l}{\lambda_T}\frac{1}{\mu_0 L}. \tag{17}$$

Let us discuss these parameters. The damping α comes from the tunneling of normal electrons; we can consider it small. The ratio β of flux over flux quantum characterizes the rf-SQUID. If $\beta \gg 1$, the squid can operate in different states which are the minima of the potential. If $\beta \approx 1$, there is only one state. The new parameter κ measures the retro-action of the SQUID on the electromagnetic field; it is crucial for the effects that we discuss below. This parameter increases with the density of rings and their surface S. It is also larger for a small inductance L. The ratio of film thickness over wavelength l/λ_T should be small so that we can neglect the variation of $\mathbf{h}$ and φ in the film. Equations (15) and (16) are our principal model and we now proceed to analyze them.

III. MICROWAVE SPECTROSCOPY DATA

In this section we analyze the small signal response of the film around a given state. This state can be changed at will by applying a static magnetic field. This way one can tune the resonant frequency of the film; this a big advantage of these rf-SQUIDs.

As in [13] we assume that the film is submitted to a stationary field $\mathbf{h}_s$ that will fix the phase φ_s. We can then linearize Eqs. (15) and (16) around this state and write

$$\mathbf{h} = \mathbf{h}_s + \delta\mathbf{h}, \quad \varphi = \varphi_s + \delta\varphi,$$

where the field $\delta\mathbf{h}$ and the variable $\delta\varphi$ are small. Their evolution is given by

$$\delta\mathbf{h}_{,\tau\tau} - \delta\mathbf{h}_{,\zeta\zeta} = \kappa(\delta\mathbf{h}_{,\tau\tau}\cdot\mathbf{n} + \delta\varphi_{,\tau\tau})\delta(\zeta)\mathbf{n}, \tag{18}$$

$$\delta\varphi_{,\tau\tau} + \alpha\delta\varphi_{,\tau} + \delta\varphi + \beta\cos\varphi_s\delta\varphi = -\delta\mathbf{h}\cdot\mathbf{n}. \tag{19}$$

To solve Eqs. (18) and (19) we assume the usual harmonic dependence

$$\delta\mathbf{h} = e^{i\omega t}\mathbf{f}, \quad \delta\varphi = e^{i\omega t}\phi.$$

This yields the following equations:

$$\mathbf{f}_{,\zeta\zeta} + \omega^2\mathbf{f} = \omega^2\kappa\,(\mathbf{f}\cdot\mathbf{n} + \phi)\,\delta(\zeta)\mathbf{n}, \tag{20}$$

$$\phi\left(\omega_r^2 - \omega^2 + \alpha i\omega\right) = -\mathbf{f}\cdot\mathbf{n}, \tag{21}$$

where we have introduced the resonant frequency ω_r:

$$\omega_r^2 = 1 + \beta\cos\varphi_s. \tag{22}$$

We now set up the scattering experiment by assuming an incident field and calculating the reflected and transmitted fields. For $\zeta < 0$ we have

$$\mathbf{f}_-(\zeta) = \mathbf{f}_{\text{in}}e^{-i\omega\zeta} + \mathbf{f}_{\text{r}}e^{i\omega\zeta}. \tag{23}$$

For $\zeta > 0$ the field is

$$\mathbf{f}_+(\zeta) = \mathbf{f}_{\text{tr}}e^{i\omega\zeta}. \tag{24}$$

At the interface $\zeta = 0$, $\mathbf{f}$ is continuous so that

$$\mathbf{f}_{\text{in}} + \mathbf{f}_{\text{r}} = \mathbf{f}_{\text{tr}}. \tag{25}$$

We have the following jump condition for $\mathbf{f}_\zeta$:

$$[\mathbf{f}_\zeta]_{0_-}^{0_+} = \kappa\omega^2(\mathbf{f}_{\text{tr}}\cdot\mathbf{n} + \phi)\mathbf{n}. \tag{26}$$

This yields

$$\mathbf{f}_{\mathbf{in}} - \mathbf{f}_{\mathbf{r}} = \mathbf{f}_{\text{tr}} - i\omega\kappa(\mathbf{f}_{\text{tr}}\cdot\mathbf{n} + \phi)\mathbf{n}. \tag{27}$$

From Eqs. (25) and (27) it follows

$$\mathbf{f}_{\mathbf{in}} = \mathbf{f}_{\text{tr}} - i\frac{\omega\kappa}{2}\mathcal{M}(\omega)(\mathbf{f}_{\text{tr}}\cdot\mathbf{n})\mathbf{n}, \tag{28}$$

$$\mathbf{f}_{\mathbf{r}} = i\frac{\omega\kappa}{2}\mathcal{M}(\omega)(\mathbf{f}_{\text{tr}}\cdot\mathbf{n})\mathbf{n}, \tag{29}$$

where

$$\mathcal{M}(\omega) = 1 + \left(\omega^2 - \omega_r^2 - i\alpha\omega\right)^{-1}. \tag{30}$$

From the first equation we obtain

$$(\mathbf{f}_{\text{tr}}\cdot\mathbf{n}) = D(\omega)(\mathbf{f}_{\text{in}}\cdot\mathbf{n}), \tag{31}$$

where

$$D(\omega) = \left[1 - i\frac{\omega\kappa}{2}\mathcal{M}(\omega)\right]^{-1}. \tag{32}$$

Using these expressions we obtain

$$\mathbf{f}_{\mathbf{r}} = i\frac{\omega\kappa}{2}\mathcal{M}(\omega)D(\omega)(\mathbf{f}_{\text{in}}\cdot\mathbf{n})\mathbf{n}, \tag{33}$$

$$\mathbf{f}_{\mathbf{tr}} = \mathbf{f}_{\text{in}} + i\frac{\omega\kappa}{2}\mathcal{M}(\omega)D(\omega)(\mathbf{f}_{\text{in}}\cdot\mathbf{n})\mathbf{n}. \tag{34}$$

Equation (33) implies that the polarization of the reflected wave is determined by $\mathbf{n}$ only. On the other hand the direction of the transmitted wave depends on the orientations of $\mathbf{n}$ and $\mathbf{f}_{\text{in}}$ and on the frequency ω.

From expression (33) the reflection coefficient is

$$\mathcal{R} = \frac{|\mathbf{f}_{\mathbf{r}}|^2}{|\mathbf{f}_{\mathbf{in}}|^2} = \frac{(\omega\kappa/2)^2|\mathcal{M}(\omega)|^2\cos^2\theta}{1 + (\omega\kappa/2)^2|\mathcal{M}(\omega)|^2}, \tag{35}$$

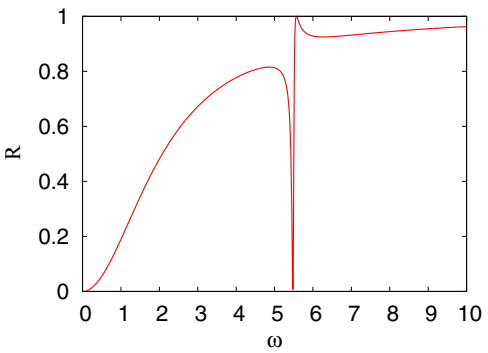

FIG. 2. (Color online) The reflection coefficient $\mathcal{R}(\omega)$ from (35) for a plane wave normally incident to the film; $\theta = 0$.

where θ is defined by the formula

$$\mathbf{f}_{\text{in}}\cdot\mathbf{n} = |\mathbf{f}_{\text{in}}|\cos\theta. \tag{36}$$

The transmission coefficient is $\mathcal{T} = |\mathbf{f}_{\mathbf{tr}}|^2/|\mathbf{f}_{\mathbf{in}}|^2$. It is

$$\begin{aligned}\mathcal{T} &= 1 - \frac{(\omega\kappa/2)^2|\mathcal{M}(\omega)|^2\cos^2\theta}{1 + (\omega\kappa/2)^2|\mathcal{M}(\omega)|^2}\cos^2\theta \\ &\quad + i\frac{\omega\kappa}{2}\frac{[\mathcal{M}(\omega) - \mathcal{M}^*(\omega)]}{1 + (\omega\kappa/2)^2|\mathcal{M}(\omega)|^2}\cos^2\theta \\ &= 1 - \mathcal{R} - \frac{\omega\kappa\,\mathrm{Im}\mathcal{M}(\omega)}{1 + (\omega\kappa/2)^2|\mathcal{M}(\omega)|^2}\cos^2\theta.\end{aligned} \tag{37}$$

Let us analyze numerically the reflection and transmission coefficients. We choose $\beta = 30$ so that we are in the highly hysteretical case as in [13]. Figure 2 shows the dependance of the reflection coefficient on ω for a normal incidence in the lossless case $\alpha = 0$, when $\kappa = 1$ and $\beta = 30$. The external magnetic field h_s is assumed to be zero. Then we can take $\varphi_s = 0$ which is the global minima of the potential of Eq. (16) (see Fig. 2 in [13]). The reflection coefficient shows a strong resonance for frequencies near ω_r; this resonance is of the Fano type (see [16]). The value of the resonance frequency is

$$\omega_r = \sqrt{1 + \beta\cos\phi_s} \approx 5.56.$$

The metasurface is transparent for small ω, when the frequency is large the incident field is totally reflected. The shape of the spectrum does not depend on the specific value of β and ω_r. For instance, the experimentalists [12] chose a smaller β and obtained a reflection coefficient that behaves similarly to the one shown in Fig. 2.

The magnetic component of the reflected wave is always oriented in the direction of the normal. On the contrary, the polarization angle of the transmitted wave $\mathbf{f}_{\mathbf{tr}}$ depends on the frequency ω and on the orientation of the split ring (angle θ). To analyze this dependance, assume that the incident field is in the plane defined by the normal vector $\mathbf{n}$ and the unit vector $\mathbf{z}$; this will give the main effect. We will also assume the incident field to be parallel to $\mathbf{y}$:

$$\mathbf{f}_{\text{in}} = \begin{pmatrix}0\\1\\0\end{pmatrix}.$$

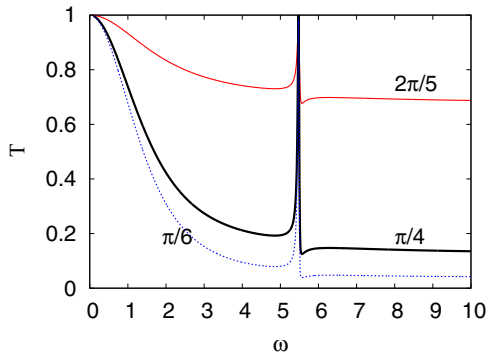

FIG. 3. (Color online) The transmission coefficient $\mathcal{T}(\omega)$ from (37) for a plane wave and three values of the orientation angle θ.

Then the reflected and transmitted fields can be written as

$$\mathbf{f}_{\rm r} = \begin{pmatrix} 0 \\ R_1 \\ R_2 \end{pmatrix}, \quad \mathbf{f}_{\rm tr} = \begin{pmatrix} 0 \\ T_1 \\ T_2 \end{pmatrix}.$$

From the relations (30), (32), (33), (34) we get

$$R_1 = T_1 - 1, \quad R_2 = T_2, \tag{38}$$

$$T_1 = D(\omega)\left[1 - i\frac{\kappa\omega}{2}\sin^2\theta\mathcal{M}(\omega)\right],$$
$$T_2 = -\frac{i\kappa\omega\sin\theta\cos\theta}{2}D(\omega)\mathcal{M}(\omega). \tag{39}$$

The transmission coefficient $\mathcal{T}(\omega)$ is shown in Fig. 3 for three different values of the orientation angle $\theta = 2\pi/5$, $\pi/4$, and $\pi/6$.

Note that the array is transparent $\mathcal{T} = 1$ when $\omega = \omega_r$. Past this frequency, the transmission coefficient asymptotically tends to a constant. For a large angle $\theta = 2\pi/5$, the ring has less influence, since most of the field is transmitted. When the angle is reduced, the incoming magnetic field interacts strongly with the rf-SQUIDs so the reflected field is stronger.

From the expression (39) for $T_{1,2}$ one obtains the angle of the polarization of the transmitted wave ψ in the (y,z) plane:

$$\psi = \arctan\left(\frac{\mathrm{Re}T_2}{\mathrm{Re}T_1}\right). \tag{40}$$

Figure 4 shows this angle ψ as a function of ω and θ.

Figure 4 demonstrates the Faraday effect which takes place in the rf-SQUID metasurface under consideration. The polarization rotation angle ψ depends both on the frequency ω and on the inclination angle of the rf-SQUIDs. The angle of rotation of the polarization changes sharply near the resonant frequency ω_r (gigantic Faraday effect). This angle depends strongly on θ; it has a pronounced resonance character near ω_r. In this case, when θ changes from $-\pi/2$ to 0 angle ψ monotonically decrease from 0 to $-\pi/2$. For $\theta = 0$ the angle ψ jumps from $-\pi/2$ to $\pi/2$ and monotonically decreases to 0 when θ changes from 0 to $\pi/2$ (see Fig. 4). Introducing losses which are always present in any practical situation smooths the jump transition, Fig. 5. We remark that the values of the angle are different below and above the resonance. The conducting

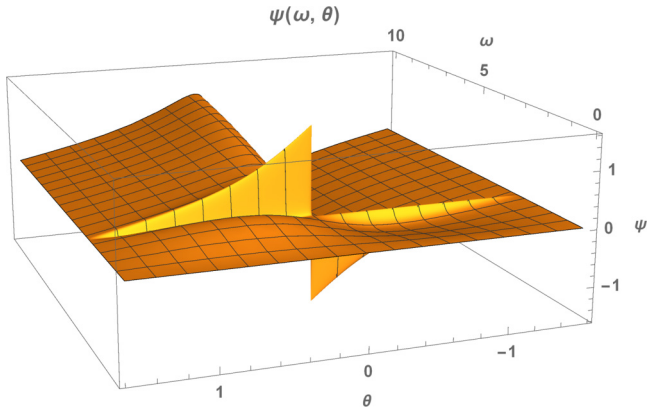

FIG. 4. (Color online) Angle $\psi(\omega)$ from (40) as a function of ω and θ; $\alpha = 0$.

rings of [3] give the same angles below and above resonance. This difference is probably due to different field-film coupling in the two systems; we have a Fano resonance while Kodera *et al.* have a standard resonance.

IV. DETAILED STUDY OF THE RESONANCE

We study here the characteristics of the resonance of the coupled system: rf-SQUID and field. From Eqs. (19) and (34) we can write the time-dependent phase equation as [7]

$$\ddot{\varphi}(t) + \alpha\dot{\varphi}(t) + (1 + \beta\cos\phi_s)\varphi(t) = -f(t),$$
$$f(t) = \frac{\kappa}{2}[\dot{\varphi}(t) + \dot{f}(t)] + k\cos\omega t. \tag{41}$$

Recalling the resonant frequency ω_r from (22) we replace

$$\cos\omega t \mapsto \exp(i\omega t),$$

so that the system (41) can be rewritten; the solutions of the resulting system have the following form:

$$\varphi(t) = A\exp(i\omega t), \quad f(t) = B\exp(i\omega t),$$
$$A = -kC^{-1}, \quad B = k\left[\left(\omega_r^2 - \omega^2\right) + i\alpha\omega\right]C^{-1},$$
$$C = \omega_r^2 - \omega^2\left(1 - \frac{\kappa}{2}\alpha\right) + i\omega\left[\alpha + \frac{\kappa}{2}\left(1 + \omega^2 - \omega_r^2\right)\right].$$

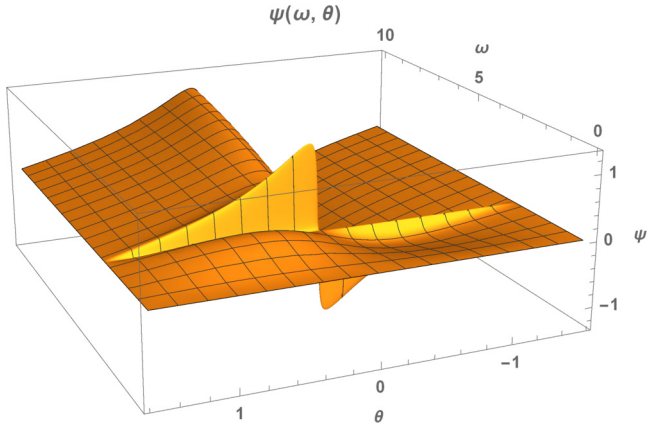

FIG. 5. (Color online) Angle $\psi(\omega)$ from (40) as a function of ω and θ; $\alpha = 0.05$.

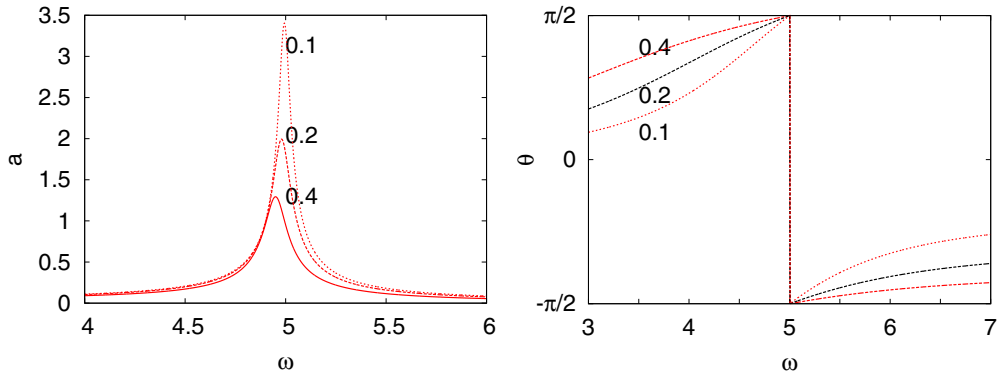

FIG. 6. (Color online) Plot of the amplitude $a(\omega)$ (left panel) and the phase $\theta(\omega)$ (right panel) for three different values of the coupling $\kappa = 0.4, 0.2$, and 0.1. The other parameters are $\omega_r = 5, \alpha = 0.01$.

Representing A in terms of a phase and an amplitude $A = a\exp(i\theta)$ we obtain

$$a = \frac{k}{\sqrt{\left\{\omega_r^2 - \omega^2[1-(\kappa\alpha/2)]\right\}^2 + \omega^2\left[\alpha + (\kappa/2)\left(1+\omega^2-\omega_r^2\right)\right]^2}},$$

$$\tan\theta = \frac{\omega\left[\alpha + (\kappa/2)(1+\omega^2-\omega_r^2)\right]}{\omega^2[1-(\kappa\alpha/2)] - \omega_r^2}.$$

The amplitude a and the phase θ are plotted as a function of the frequency ω in Fig. 6. Notice how the resonance gets sharper for a small coupling κ. We also have the typical jump in the phase as one crosses the resonance.

The amplitude $a(\omega)$ reaches its maximal value for

$$\omega_{\max}^2 = \frac{1}{3\tilde{\kappa}^2}\left[\tilde{\kappa}^2\left(2\omega_r^2 - \alpha^2 - 2\right) - 1\right] + \frac{1}{3\tilde{\kappa}^2}\Big[1 + \tilde{\kappa}^2\Big(4 + 2\omega_r^2 - \alpha^2 - 6\tilde{\kappa}\alpha + \tilde{\kappa}^2\left\{\left(\omega_r^2-1\right)\left[\left(\omega_r^2-1\right) - 4\alpha^2\right] + \alpha^4\right\}\Big)\Big]^{1/2}, \quad (42)$$

where $\tilde{\kappa} = \kappa/2$. Since α and $\tilde{\kappa}$ are small, $\omega_{\max}^2$ up to second order has following form:

$$\omega_{\max}^2 \approx \omega_r^2 - \frac{\alpha^2}{2} - \alpha\tilde{\kappa} - \left(\omega_r^2 + \frac{1}{2}\right)\tilde{\kappa}^2.$$

When ω is close to ω_r ($\omega = \omega_r + \Delta$, $|\Delta| \ll 0$) and α and κ are small, then

$$a \approx \frac{k}{\omega_r\sqrt{4\Delta^2 + (\alpha+\tilde{\kappa})^2}}. \quad (43)$$

If $\kappa = 0$, we recover the classical resonance observed for a damped driven linear oscillator, both for θ and a [17].

V. CONCLUSION

We analyzed the interaction of a plane electromagnetic wave with a two-dimensional array of rf-SQUIDs. The wave vector of the incident field is assumed orthogonal to the array of rf-SQUIDs. All rf-SQUIDs have the same inclination with respect to the surface of the array and the effective thickness of this "array film" is much smaller then the wavelength. Our main result is that despite this small thickness, the array effectively controls the wave reflection and transmission. In particular, it changes the polarization of the reflected wave and this change is determined only by the orientation of the rf-SQUIDs. This effect is identical to the Kerr effect in a gyrotropic medium. Here the gyrotropy is introduced by the rf-SQUIDs. The polarization of the transmitted wave also changes and depends both on the carrier frequency and on the inclination angle of the rf-SQUIDs. This is similar to a Faraday effect. At the resonance frequency we obtain a gigantic Faraday effect. We emphasize that the thickness of the array is always much smaller than the wavelength.

This array of rf-SQUIDs acts as a metasurface that controls the polarization of an electromagnetic wave. This control can be changed using a static magnetic field and this is a unique property of these films. Also they operate at low temperature so there is very little dissipation.

The analysis that we carried out is limited by the linear approximation. Increasing the incident field will cause a larger current in the ring and subsequently a nonlinear response of the rf-SQUIDs. We then expect nonlinear Kerr and Faraday effects combined with bistability.

ACKNOWLEDGMENTS

The research of A.I.M. was supported by the Russian Science Foundation (Project No. 14-22-00098). The research of I.R.G. was partially supported by the Ministry of Education and Science of the Russian Federation (Project DOI: RFMEFI58114X0006). J.G.C. thanks the Region Haute-Normandie for support through a research grant GRR-LMN and the CRIHAN computing center for the use of its facilities.

[1] N. Yu *et al.*, Light propagation with phase discontinuities: Generalized laws of reflection and refraction, Science **334**, 333 (2011).

[2] X. Ni *et al.*, Broadband light bending with plasmonic nanoantennas, Science **335**, 427 (2012).

[3] T. Kodera, D. L. Sounas, and C. Caloz, Artificial Faraday rotation using a ring metamaterial structure without static magnetic field, Appl. Phys. Lett. **99**, 031114 (2011).

[4] N. Lazarides, G. P. Tsironis, and M. Eleftheriou, Dissipative discrete breathers in rf SQUID metamaterials, Nonlinear Phenom. Complex Syst. **11**, 250 (2008).

[5] N. Lazarides and G. P. Tsironis, rf superconducting quantum interference device metamaterials, Appl. Phys. Lett. **90**, 163501 (2007).

[6] G. P. Tsironis, N. Lazarides, and M. Eleftheriou, Dissipative breathers in rf SQUID metamaterials, *PIERS Proceedings 2009* (Beijing, China, 2009), pp. 52–56.

[7] A. I. Maimistov, I. Gabitov, Nonlinear response of a thin metamaterial film containing Josephson junctions, Opt. Commun. **283**, 1633 (2010).

[8] Chunguang Du, Hongyi Chen, and Shiqun Li, Quantum left-handed metamaterial from superconducting quantum-interference devices, Phys. Rev. B **74**, 113105 (2006).

[9] S. M. Anlage, The physics and applications of superconducting metamaterials, J. Opt. **13**, 024001 (2011).

[10] P. Jung, A. V. Ustinov, and S. M. Anlage, Progress in superconducting metamaterials, Supercond. Sci. Technol. **27**, 073001 (2014).

[11] M. Trepanier, Daimeng Zhang, O. Mukhanov, and S. M. Anlage, Realization and modeling of metamaterials made of rf superconducting quantum-interference devices, Phys. Rev. X **3**, 041029 (2013).

[12] P. Jung, S. Butz, S. V. Shitov, and A. V. Ustinov, Low-loss tunable metamaterials using superconducting circuits with Josephson junctions, Appl. Phys. Lett. **102**, 062601 (2013).

[13] J.-G. Caputo, I. Gabitov, and A. I. Maimistov, Electrodynamics of a split-ring Josephson resonator in a microwave line, Phys Rev. B **85**, 205446 (2012).

[14] The $,t$ subscript denotes the time partial derivative. In the rest of the article we will use this notation to simplify the expressions.

[15] A. Barone and G. Paterno, *Physics and Applications of the Josephson Effect* (John Wiley & Sons, New York, 1982).

[16] A. E. Miroshnichenko, S. Flach, and Y. S. Kivshar, Fano resonances in nanoscale structures, Rev. Mod. Phys. **82**, 2257 (2010).

[17] L. Landau and E. Lifchitz, *Cours de Physique Théorique, Mecanique* (Mir, Moscou, 1966).